Reaction Mechanism in Inelastic Scattering of Protons from Mg, Cr, and Other Elements from 3.5 to 7 Mev*

FREDERICK D. SEWARD†
University of Rochester, Rochester, New York
(Received November 26, 1958)

Inelastic scattering of protons leading to the first excited states of Mg^{24} and Cr^{52} and to single excited states of other elements has been studied. $d\sigma/d\omega$ (90°) was measured as a function of proton energy from 3.5 to 7 Mev. Angular distributions of inelastically scattered protons and $p'-\gamma$ angular correlations were taken at several energies. Experimental measurements are compared with direct-interaction theory and with predictions of the statistical model. Data for $Cr^{52}(p,p')Cr^{52*}$ at 5.4 Mev is well fit by the statistical model. The $Mg^{24}(p,p')Mg^{24*}$ reaction at 7 Mev can be interpreted as a direct interaction. The Mg reaction at 5.4 Mev and the Cr reaction at 7 Mev appear to have a bit of direct interaction in them. It is suggested that the amount of direct interaction in this (p,p') reaction depends on the nuclear barrier height. Statistical-model expressions for reactions studied are given in an Appendix.

I. INTRODUCTION

THE concept of a compound nucleus (CN) has been quite useful in explaining many of the features of low-energy nuclear reactions. When many levels of the CN are excited in a reaction, the statistical model[1] is expected to predict its behavior. Many reactions in which this model should be valid do not show the expected behavior.[2,3] These have been interpreted as direct interactions (DI). Deuteron stripping reactions are perhaps the most familiar examples of direct interactions.

The statistical model is based on three assumptions: (1) The CN assumption—the incident particle and the target nucleus immediately form a compound state in which the incident energy is shared among all nucleons. The disintegration of this compound state is independent of its mode of formation. (2) Many CN states contribute to the reaction at the energy considered. (3) The statistical assumption—the phases of the wave functions describing these states are essentially random. As a consequence of this last assumption, angular distributions of reaction products are symmetrical about 90°. Angular correlations between inelastic protons and subsequent γ rays are expected to show no particular axis of symmetry.[4]

If the CN assumption does not hold, and the incident particle interacts with only one or a few nucleons of the target nucleus, the reaction is called a DI. The simplest DI model is based on three assumptions: (1) The Born approximation is made. (2) The entire reaction is assumed to take place in a region close to the nuclear surface. (3) The range of the nucleon-nucleon interaction is taken to be zero. Angular distributions based on this simple model have the form of spherical Bessel functions.[5] Angular correlations between inelastic particles and subsequent γ rays are symmetrical about the direction of the recoil nucleus. If the γ radiation is pure electric quadrapole ($E2$), and if θ_γ is the angle measured from the recoil nucleus direction, the angular correlation has the form $\sin^2(2\theta_\gamma)$. Angular distributions from some α-particle reactions are well fitted by this simple model.[6,7]

A more sophisticated DI calculation in which the above three assumptions were dropped has been done by Levinson and Banerjee.[8] Optical-model wave functions were used for incident and scattered waves and shell-model wave functions for the initial and final states. A finite-range Yukawa force was assumed to act between nucleons and the calculation was done throughout the nuclear volume. The variable parameters in this calculation were picked to give agreement with the $C^{12}(p,p'\gamma)$ data at 14–18 Mev. Calculated angular distributions are quite sensitive to distortion and bear no resemblance to spherical Bessel functions. Predicted $p'-\gamma$ angular correlations, however, are quite similar to those of Born approximation and have the form $A+B\sin^2[2(\theta_\gamma-\theta_0)]$, with A, B, and θ_0 constants. This model gives a reasonable fit to a wide range of data.

Since the lifetime of a CN is quite long compared with the time required for a DI, these two processes are expected to be incoherent.[9]

The experimental work to be discussed in this paper is concerned only with inelastic proton scattering leaving the target nucleus in a single, definite excited state, usually the first. This nucleus subsequently decays by emitting a γ ray. Three types of data were

* This work supported by the U. S. Atomic Energy Commission and by The Research Corporation.
† Present address: University of California Radiation Laboratory, Livermore, California.
[1] D. C. Peaslee, *Annual Review of Nuclear Science* (Annual Reviews, Inc., Stanford, 1955), Vol. 5, p. 99.
[2] R. Sherr, *Proceedings of the University of Pittsburgh Conference on Nuclear Structure, 1957*, edited by S. Meshkov (University of Pittsburgh and Office of Ordnance Research, U. S. Army, 1957), p. 361.
[3] L. R. B. Elton and L. C. Gomes, Phys. Rev. **105**, 1027 (1957).
[4] G. R. Satchler, Phys. Rev. **94**, 1304 (1954).
[5] G. R. Satchler, Proc. Phys. Soc. (London) **A68**, 1037 (1955).
[6] H. J. Watters, Phys. Rev. **103**, 1763 (1956).
[7] C. S. Hunting and N. S. Wall, Phys. Rev. **108**, 901 (1957).
[8] C. A. Levinson and M. K. Banerjee, Ann. Phys. N. Y. **2**, 471 (1957); **3**, 67 (1958).
[9] A. M. Lane, Revs. Modern Phys. **29**, 191 (1957).

taken. Measurements were made of $d\sigma/d\omega$ (90°) as a function of incident proton energy, angular distributions of the inelastic protons, and angular correlations between the inelastic protons and γ rays.

Relatively thick targets were used so that many levels of the CN would contribute to the reaction and the statistical model could be applied to the results. Targets were about 150 kev thick at the energies used. The data of Shiffer *et al.*[10] indicate that at least 7 levels of the CN contribute to the reaction at any one energy for $Z\sim25$. The CN level spacing is quite large in the lighter elements and resonant effects appear in some of the data. For these elements, measurements were taken at energies between resonances so the ratio of CN to DI components of the reaction would be as low as possible. Some data for $Mg^{24}(p,p'\gamma)$ were taken directly on what appeared to be a resonance to see what effect this had on the angular correlations.

Predictions of the statistical model are compared with the $Cr^{52}(p,p'\gamma)$ data. The statistical model is applied to total cross-section measurements and angular distributions of inelastic protons in the form developed by Hauser and Feshbach.[11] Predictions for angular correlations were obtained from general expressions given by Devons and Goldfarb.[12] Nuclear properties appear in these formulas in the form of transmission coefficients, T_L, where L is the orbital angular momentum of the proton. It was assumed that only two channels were open for the CN decay: the elastic channel, and inelastic scattering to the first excited state. Expressions of this type have been calculated by Satchler[4,13] but the published formulas contain errors. These have been recalculated and are given in the Appendix. Two models were used to calculate the T_L. A black nucleus (continuum theory) was first assumed since tables[14] were available from which the T_L could be easily obtained. Fits to the data with this model were not good so some T_L were calculated using an optical-model potential.

The simple Born approximation DI theory is compared with some of the angular distributions taken. No distorted wave calculations of angular distributions were made. The form of the angular correlations, however, is not supposed to be much affected by distortion and some of the data are fitted with the predicted $A+B\sin^2[2(\theta_\gamma-\theta_0)]$ form.

II. EXPERIMENTAL METHOD

The University of Rochester 27 in. variable-energy cyclotron was used to make the measurements to be described. The internal beam is extracted electrostatically, focused by a pair of quadrapole magnets, analyzed by a wedge magnet, and passes through two scattering chambers. A 10-in. diameter chamber can be used in conjunction with a 180° spectrometer magnet for high-resolution work or the beam can be passed through this 10-in. chamber and into a 36-in. diameter chamber containing two counters on rotating arms. The energy calibration of the beam was accurate to about 0.5% and the full width at half maximum of the analyzed beam in energy was less than 0.5%. This energy spread in the beam was small compared to the target thickness used and was usually neglected.

Targets used were mostly self-supporting natural metal foils about 2 mg/cm^2 thick. The Be target had been made for a previous experiment. The C target was made by cracking acetylene gas on a hot Ta plate.[15] Commercial Al, Ti, and Au foils were used.[16] Mg, V, and Fe targets were made by reducing commercial foils in thickness by electropolishing. Cr and Co foils were made by electroplating, and the Si target was made from a thin piece of Pyrex glass.

Inelastic protons from these targets were detected by a scintillation counter in the 36-in. chamber. This counter consisted of a 0.020-in. CsI(Tl) crystal bonded to the face of a DuMont-6291 photomultiplier. Electronics were conventional and pulses from this counter were analyzed in a RIDL model 3300 100-channel pulse-height analyzer.

The cross section at 90° was measured by fixing this counter at 90° and an ion chamber monitor at 23°. Scattering into this monitor was essentially all elastic and is known to be Coulomb for $Z\geq13$ at these energies.[17,18] Elastic scattering from Au is Coulomb at all angles.[17] Protons were scattered from both a Au target and the target of interest. If it is assumed that elastic scattering from the target of interest is Coulomb at the monitor angle, the inelastic scattering cross section in mb/sterad is given by

$$\frac{d\sigma}{d\omega}(90°)=5.184\frac{Z^2M(\mathrm{Au})N(T)}{sN(\mathrm{Au})M(T)E_p^2}.$$

Z is the atomic number of the target of interest and s is the abundance of the isotope which contributes the inelastic group. $N(T)$ is the number of counts in this group and $M(T)$ is the number of monitor counts. $N(\mathrm{Au})$ and $M(\mathrm{Au})$ are the number of counter and monitor counts from the Au target. E_p is proton energy in the laboratory system. This measurement of cross section is independent of the monitor angle, beam

[10] J. P. Schiffer *et al.*, Phys. Rev. **104**, 1661 (1956).
[11] W. Hauser and H. Feshbach, Phys. Rev. **87**, 366 (1952).
[12] S. Devons and L. J. B. Goldfarb, *Handbuch der Physik* (Springer-Verlag, Berlin, 1957), Vol. 42, 362.
[13] G. R. Satchler, Phys. Rev. **104**, 1198 (1956).
[14] H. Feshbach *et al.*, Atomic Energy Commission Report NYO-3077, 1953 (unpublished).
[15] G. C. Phillips and J. E. Richardson, Rev. Sci. Instr. **21**, 885 (1950).
[16] Thanks are due to Mr. L. A. Hurwitz and the Hamilton Watch Company for supplying the Ti foil.
[17] W. F. Waldorf and N. S. Wall, Phys. Rev. **107**, 1602 (1957).
[18] C. A. Preskitt, Jr., and W. P. Alford, Atomic Energy Commission Report NYO-2172, 1958 (unpublished); also Phys. Rev. (to be published).

current, and target thickness. Center-of-mass corrections are negligible at these energies. For these measurements targets made an angle of 45° with the beam and transmissive geometry was used. The above expression was used to compute the inelastic cross section.

Angular distributions were taken with this same scintillation counter. Another scintillation counter was used as a monitor at 45°. Targets made an angle of ±30° with the beam. The target chamber was aligned so the beam passed through the center of the target by placing a fluorescent screen in the target position and observing the beam spot with a telescope. The counter geometry and zero of the angle scale were checked by measuring the scattering from a Au target. This was found to be Coulomb within counting statistics of 3%.

$p'-\gamma$ angular correlations were taken in the 10-in. scattering chamber. Part of one side of this chamber is $\frac{1}{16}$-in. thick brass so γ rays produced in the target can be detected outside the chamber with attenuation in the chamber walls a minimum. The γ detector used was a 1-in. by $1\frac{1}{2}$-in. diameter NaI(Tl) crystal mounted on a DuMont-6292 photomultiplier. This counter was placed on a platform outside the chamber. An angle scale was marked on the platform and the γ counter could be positioned with an accuracy of ±1° by sliding it around on the platform. The geometry was checked by placing a Co^{60} source in the target position and was found to be satisfactory. The 180° spectrometer magnet was used to detect inelastically scattered protons. Slits at the magnet exit were removed, giving it an energy resolution of about 2%. Inelastic proton groups used were quite intense and there was no trouble in locating these groups or in keeping the peak of the group on the detector at the magnet exit while taking these measurements.

A fast-slow coincidence analyzer was used to take time coincidences between these inelastic protons and γ-rays. The coincidence tubes were 6BN6's. The fast coincidence circuit was adjusted to a resolving time of 30 mμsec. Two single-channel pulse-height analyzers provided energy discrimination in the slow coincidence circuit which had a resolving time of 1.5 μsec.

It was necessary to delay the γ-ray pulses since it took some time for the inelastically scattered protons to travel through the spectrometer magnet. The optimum delay was about 70 mμsec and was found by measuring the number of coincidences as a function of delay. Random coincidence rates were measured by

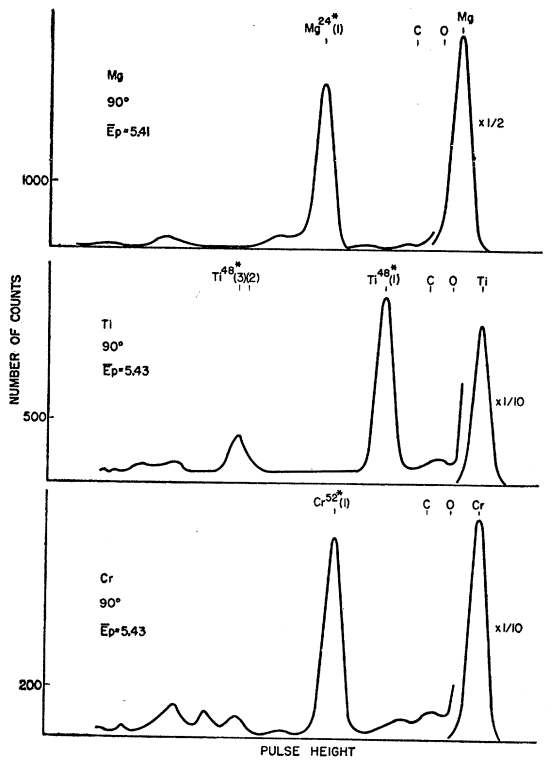

FIG. 1. Scintillation counter spectra of 5.4-Mev protons scattered from Mg, Ti, and Cr targets. Prominent groups caused by elastic and inelastic scattering from the target element are labeled. The expected position of elastic scattering from C and O contamination is also indicated. Only smooth curves drawn through the 100-channel analyzer points are shown.

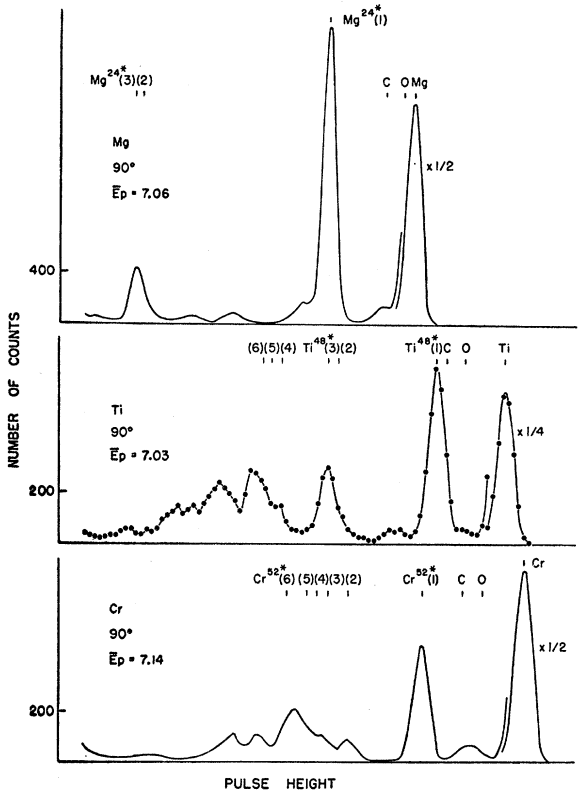

FIG. 2. Scintillation counter spectra of 7-Mev protons scattered from Mg, Ti, and Cr targets. Proton energies given are lab energies in the center of the target. Points giving the number of counts in each channel are shown for the Ti target to illustrate the way in which the curves shown in Figs. 1 and 2 were drawn.

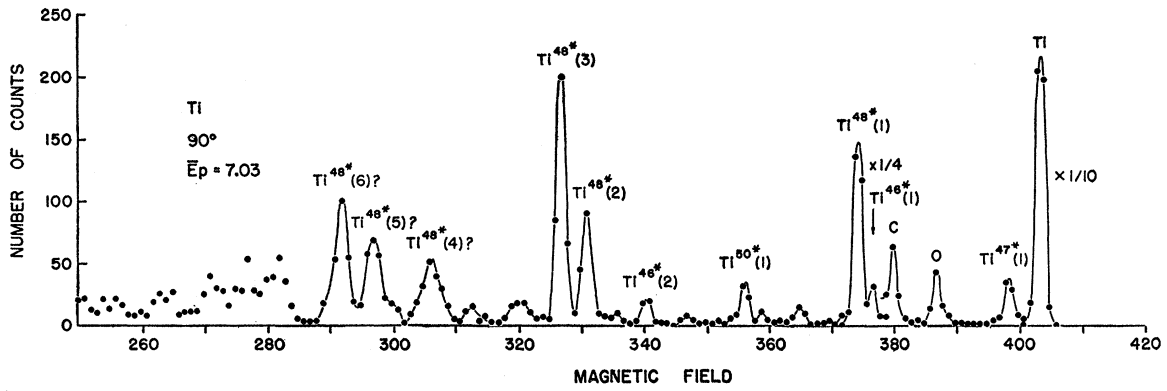

FIG. 3. Proton spectrum from the Ti target taken with spectrometer magnet. 4th, 5th, and 6th excited states of Ti^{48} are labeled as questionable because scattering from other Ti isotopes is strong in this region.

increasing this delay to 275 mμsec. Random coincidences in the fast-slow circuit were found to be a constant fraction of those in the slow coincidence circuit. Since about 90% of the counts in the slow coincidence circuit were random the number of random counts in the fast-slow circuit could be estimated. Counting rates used were such that the random rate in the fast-slow circuit was 10–20% of the true rate for most of the measurements. Angular correlations were taken by setting the spectrometer magnet at a given angle and measuring the number of $p'-\gamma$ coincidences as a function of the angular setting of the γ detector.

Figures 1 and 2 show typical spectra obtained with the scintillation counter. Prominent groups seen, and the expected positions of elastic scattering from C and O have been labeled. Proton energies indicated are lab energies in the center of the target and are in Mev. These curves are 100-channel analyzer data and points corresponding to the individual channels are shown for one spectrum. Only a smooth curve through these points is shown for the other spectra. To check on the interpretation of this scintillation counter data, some proton spectra were taken with the spectrometer magnet. A typical magnet spectrum is shown in Fig. 3. This is for the Ti target. The horizontal scale is the reading of the meter used to measure the spectrometer magnet field. The prominent inelastic proton groups have been labeled. Energies of the first three excited states of Ti^{48} calculated from this spectrum are 0.98, 2.34, and 2.46 Mev. This agrees with other work.[19,20]

III. RESULTS-Mg

Scintillation counter spectra similar to those shown in Figs. 1 and 2 were used to measure $d\sigma/d\omega(90°)$ and angular distributions. Only inelastic protons leaving Mg^{24} in its first excited state were studied. As can be seen from Figs. 1 and 2 this group is quite strong. What appears in the scintillation spectra as a small group just on the low-energy side of the Mg^{24} first excited state group was resolved by the spectrometer magnet into three groups. These correspond to inelastic scattering from states in Mg^{25} and Mg^{26}. The effect of this small group was always subtracted with no trouble.

$d\sigma/d\omega(90°)$ for inelastic scattering to the first excited state is shown in Fig. 4. Proton energy has been converted into the center-of-mass system. Horizontal bars show the target thickness and vertical arrows indicate energies where angular distributions were taken. The arrow labelled (MIT) represents an angular distribution taken by Gove and Stoddart.[21] This cross section is given in mb/sterad if the elastic scattering at 23° is Coulomb. If this is not so, the vertical scale is inaccurate. No attempt was made to check this since the absolute value of the $Mg^{24}(p,p')$ cross section is unimportant for this experiment. Error bars represent counting statistics. Resonant effects seem to be quite prominent in this curve and the bumps seen could be due to individual resonances since they have about the same width as the target.

Angular distributions of these inelastically scattered protons are shown in Fig. 5. Error bars represent counting statistics and uncertainties in background subtraction. At low angles a background appeared because of slit scattered low-energy particles in the beam. This appeared as a low-energy tail on the elastic peak and a subtraction was only necessary at low angles where the elastic peak was quite large. Thus the larger error bars at low angles. The dotted lines are angular distributions predicted by the Born-approximation direct-interaction theory. These are poor fits to the data. Changing the interaction radius does not help. The MIT angular distribution at 7.26 Mev is quite different in shape than the one given here at 7.01 Mev. This is not surprising since there appears to be a resonance in the reaction at this energy.

[19] *Nuclear Level Schemes*, $A=40$—$A=92$, compiled by Way, King, McGinnis, and van Lieshout, Atomic Energy Commission Report TID-5300 (U. S. Goverment Printing Office, Washington, D. C., 1955).

[20] R. M. Sinclair, Phys. Rev. **107**, 1306 (1957).

[21] H. E. Gove and H. F. Stoddart, Phys. Rev. **86**, 572 (1952).

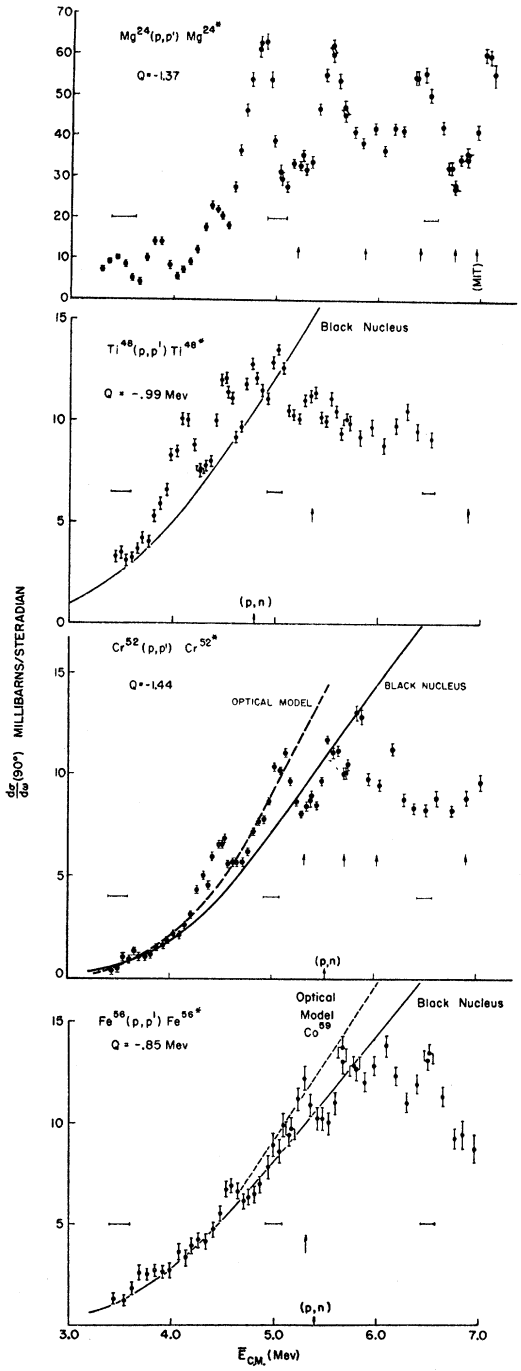

FIG. 4. $d\sigma/d\omega$ (90°) as a function of center-of-mass proton energy. Horizontal bars represent target thickness. Vertical arrows indicate energies at which angular distributions were taken and (p,n) thresholds. Solid and dashed lines are statistical-model predictions for total cross section divided by 4π.

Angular correlations are shown in Figs. 6, 7, and 8. Error bars represent counting statistics. The curves have been normalized by dividing each point by the number of single counts in the proton detector. The solid angle of the γ counter has also been taken into account so the vertical scale is in units of the γ-counter efficiency. The estimated number of random coincidences has been subtracted from each point. Several times during each measurement the delay in the γ-ray line was increased to 275 mμsec and the point was taken in the usual manner. The average of these points for each correlation is shown as a point at 5°. Within statistics this was always zero, which shows that the method of estimating random coincidences was satisfactory. The azimuthal angle between the inelastic proton and the γ ray was 180°. The direction of the recoil nucleus is indicated by a vertical arrow.

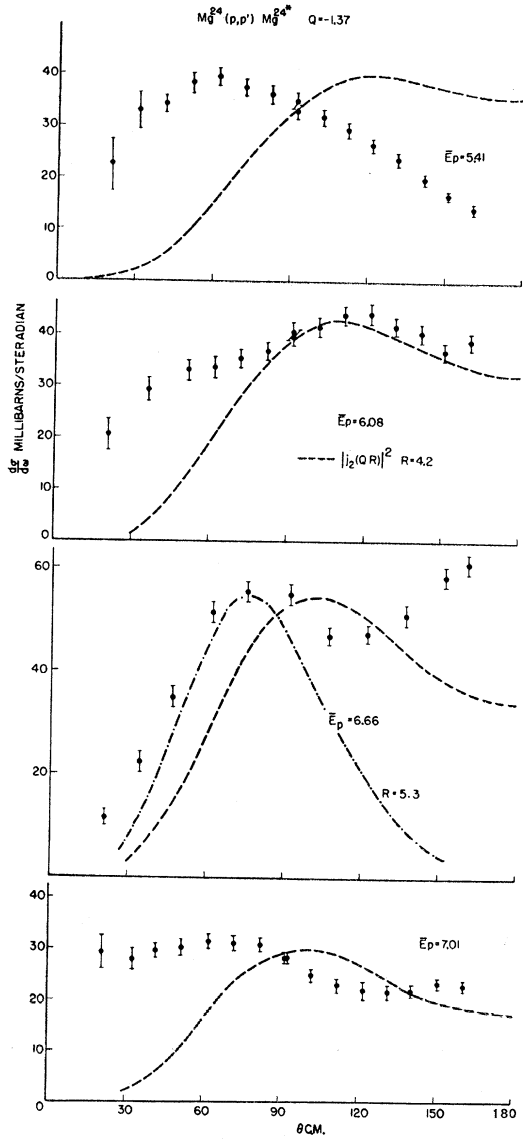

FIG. 5. Angular distribution of inelastic protons leaving Mg^{24} in its 1st excited state for proton energies indicated by arrows in Fig. 4. Dashed lines are predictions of Born-approximation direct-interaction theory. The reaction appears to have a resonance at $\bar{E}_p = 6.66$ Mev. Increasing the interaction radius does not give a better fit at this energy.

Solid curves are of the form $A+B\sin^2 2(\theta_\gamma-\theta_0)$. These curves are least-squares fits to the data. An IBM-650 computer was used to determine the best values of A and B for a given θ_0. The machine also computed the root mean square deviation of the data from the fitted curve. This calculation was repeated for several values of θ_0 and the one giving the minimum value of this root mean square deviation was taken as the best fit. This best fit is the curve which is shown.

The data at 6.66 and 7.01 Mev have been fitted by this method. The correlations at 5.41 Mev have been fitted by specifying $\theta_0=0$ and leaving some of the points out of the least-squares analysis. The three low-angle points have been omitted from the fit at $\theta_{p'}=45°$ and the two end points at $\theta_{p'}=90°$.

Consider the first three 7.01-Mev angular correlations. The axis of symmetry follows the recoil axis closely ($\theta_0=-1°$, $-5°$, $2°$ for these curves) and does not consistently coincide with the beam or inelastic proton direction. All three curves are well fit by the form which has been derived by a direct-interaction calculation at a higher energy. The values of A/B and θ_0 are of the same order as those found for the $C^{12}(p,p'\gamma)$ reaction at 16 Mev.[8] The reaction at this energy therefore might be interpreted as proceeding largely by a direct interaction, most of which goes in the forward direction.

The compound nucleus contribution to these curves is unknown so there is danger in interpreting them as a pure direct interaction, even though they have the proper form. At $\theta_{p'}=90°$, for instance, the DI symmetry axis (40° or 85°) is almost indistinguishable from that expected for the CN contribution (90°).

The Mg angular correlations at 6.66 Mev were purposely taken where the reaction shows a resonance and the CN contribution should be large. These correlations are surprisingly well fit by the DI form. However, the axis of symmetry does not follow the recoil axis as closely ($\theta_0=-16°$, $-3°$, $-5°$ for these curves) and the ratio A/B is higher. This DI form then is disturbed, but not destroyed by the resonance.

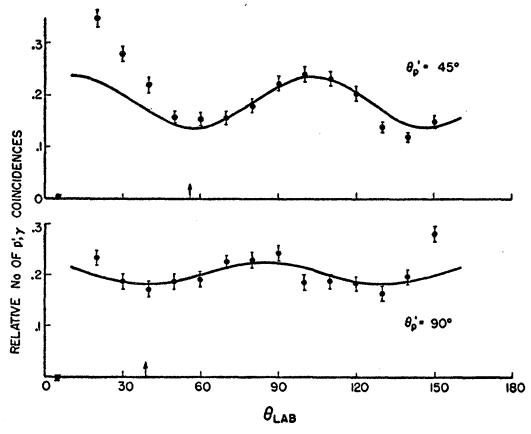

FIG. 6. $Mg^{24}(p,p'\gamma)$ angular correlations at $\bar{E}_p=5.41$ Mev. Solid curves are of the form $A+B\sin^2(2\theta_\gamma)$. Vertical arrows indicate recoil nucleus direction.

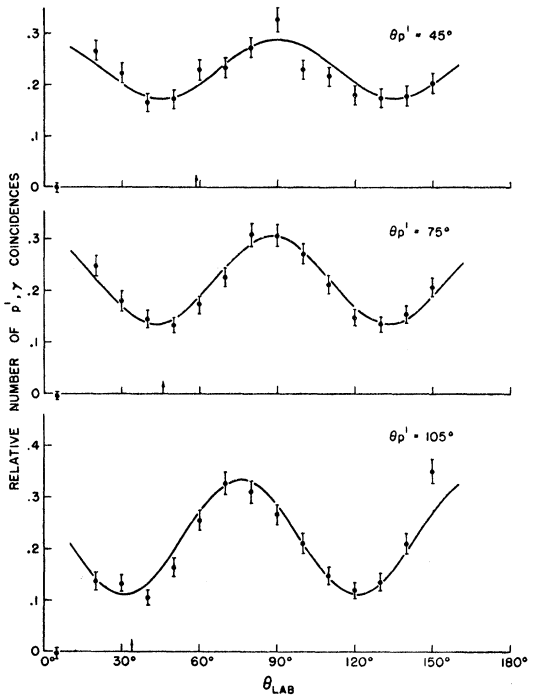

FIG. 7. $Mg^{24}(p,p'\gamma)$ angular correlations at $\bar{E}_p=6.66$ Mev. The reaction appears to have a resonance at this energy. Solid curves are of the form $A+B\sin^2[2(\theta_\gamma-\theta_0)]$. Vertical arrows indicate recoil nucleus direction.

The correlations at 5.41 Mev could be interpreted as being partially of this DI form. Once more there is danger that these symmetries are due to mostly CN formation. However, the maxima and minima fall in the places one would suspect for a DI.

The variation of $d\sigma/d\omega(90°)$ and the shape of the angular distributions with energy could indicate a large CN contribution to the reaction. No information about the DI component can be obtained from the angular distributions since the form of distorted-wave DI angular distributions has not been calculated at these energies.

IV. RESULTS-Cr

Proton spectra from the Cr target are shown in Figs. 1 and 2. The proton group corresponding to the first excited state of Cr^{52} was well resolved from all other groups of reasonable intensity. Higher excited states in Cr^{52} were not resolved in the scintillation counter spectra.

The variation of $d\sigma/d\omega(90°)$ with energy is shown in Fig. 4. Since level spacing in the compound nucleus is such that several levels should be excited at each energy, the maxima in the curve are probably due to fluctuations in the number or properties of the CN levels excited rather than to individual resonances. The (p,n)

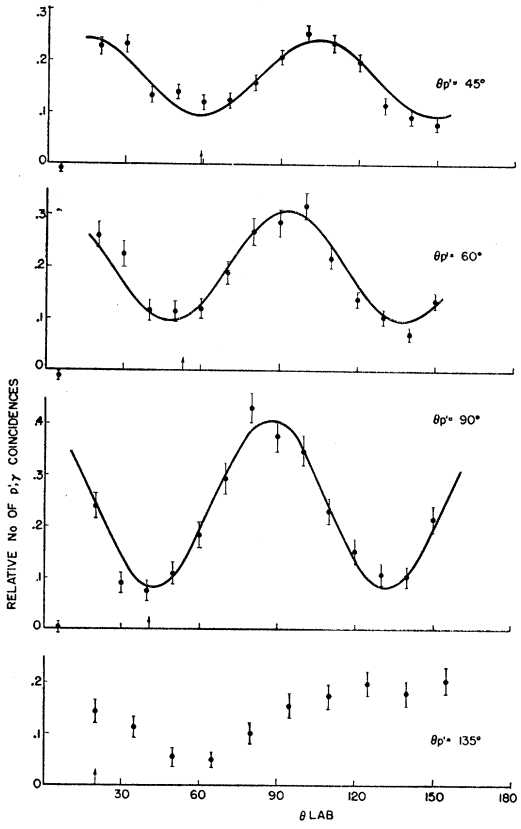

FIG. 8. $Mg^{24}(p,p'\gamma)$ angular correlations at $\bar{E}_p=7.01$ Mev. Solid curves are of the form $A+B\sin^2[2(\theta_\gamma-\theta_0)]$. Vertical arrows indicate recoil nucleus direction. See text for explanation of points at 5°.

threshold is indicated by a vertical arrow. The initial rise of cross section with energy is a barrier effect. The sudden leveling off of the cross section just above the (p,n) threshold is attributed to competition in the decay of the CN. Because angular distributions are almost isotropic, this curve can be taken as a measure of the total cross section. Error bars on the experimental points are counting statistics and the accuracy of the absolute cross-section measurement is probably better than 10%.

The solid and dotted curves in Fig. 4 have been calculated on the basis of the statistical model and under the assumption that only two channels were open for the CN decay. These curves are values of the total cross section as given by Hauser and Feshbach[11] divided by 4π (see Appendix). The solid curves are for black-nucleus penetrabilities, the dotted curves are based on optical model T_L. It has been assumed that $T_L=0$ for $L>4$ and $T_{L'}=0$ for $L'>3$. With the T_L used, this probably includes 95% of the reaction at 5.5 Mev.

All the black-nucleus penetrabilities were computed for nuclear radii $=1.45A^{\frac{1}{3}}$ fermis and for $V_0=-25$ Mev. It was not possible to use the tables for larger well depths. It can, however, be estimated that if this same radius were used with a more realistic well depth of -40 Mev, the entire curve would be lowered to about 80% of its indicated value.

Because of the two-channel assumption, these computed curves should fit the data well at low energies ($E_p<5$ Mev) and then should gradually rise above the measured cross section as inelastic scattering to higher states becomes appreciable. When the (p,n) threshold is passed, the cross section is expected to, and indeed does, drop way below the values given by this expression. It was not possible to include the higher excited states or neutron emission in the calculation since the spins of these residual levels are unknown. The continuum theory calculation for the total cross section, although a good fit at low energies, does not rise fast enough. To raise this cross section, one must either increase the radius, which already has a reasonable value, or decrease $|V_0|$, which is already unreasonably small. With a reasonable V_0 (-40 Mev) the whole curve is too low. The trouble probably either lies in the continuum assumption or in the square well used which is known to give too much reflection to fit elastic scattering data.[1]

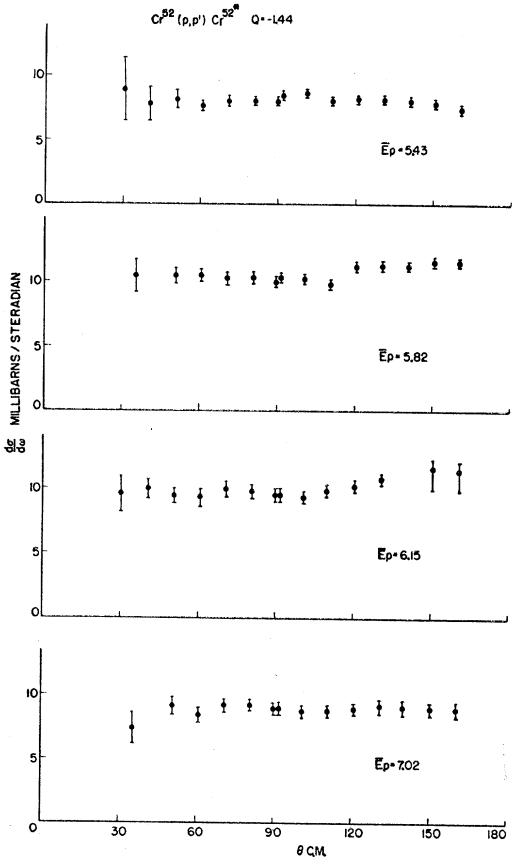

FIG. 9. Angular distribution of inelastic protons leaving Cr^{52} in its 1st excited state for proton energies indicated by arrows in Fig. 4.

Preskitt[18] has obtained good fits to angular distributions of protons elastically scattered from Co^{59} in this energy range using an optical-model potential of the form

$$\frac{V+iW}{1+\exp[(r-R)/a]}.$$

Using Preskitt's parameters as a guide, a set of T_L for Cr was calculated (on IBM 650) with $V=-50$ Mev, $W=-5$ Mev, $R=1.33A^{\frac{1}{3}}$ fermis, and $a=0.4$ fermi. (These parameters give good fits to Preskitt's data.) The dotted line in Fig. 4 is the statistical model calculation with these optical model T_L. This is a good fit to these $d\sigma/d\omega(90°)$ data for Cr.

Angular distributions taken at energies indicated in Fig. 4 by vertical arrows are shown in Fig. 9. Error bars are again counting statistics with background subtraction at the forward angles. Elastic scattering from C and O blended into the first excited state group of Cr^{52} at the back angles at 7.02 Mev. The amount of C and O on the target was determined with the spectrometer magnet and a subtraction ($\sim$10%) was made. The slight rise of $d\sigma/d\omega$ in the backward direction at 5.82 and 6.15 Mev, where no subtraction was made, may be due to C contamination.

The statistical model predicts angular distributions which are symmetrical about 90° and almost isotropic. Using optical-model T_L corresponding to a proton energy of 5.43 Mev, the predicted angular distribution is $W(\theta)=1.000+0.040P_2-0.018P_4-0.002P_6$, where $P_L=P_L(\cos\theta)$. Black-nucleus T_L give about the same result, deviations from isotropy being less than 5% for both models. The inelastic proton angular distributions of Fig. 9 then, are well fit by the statistical model.

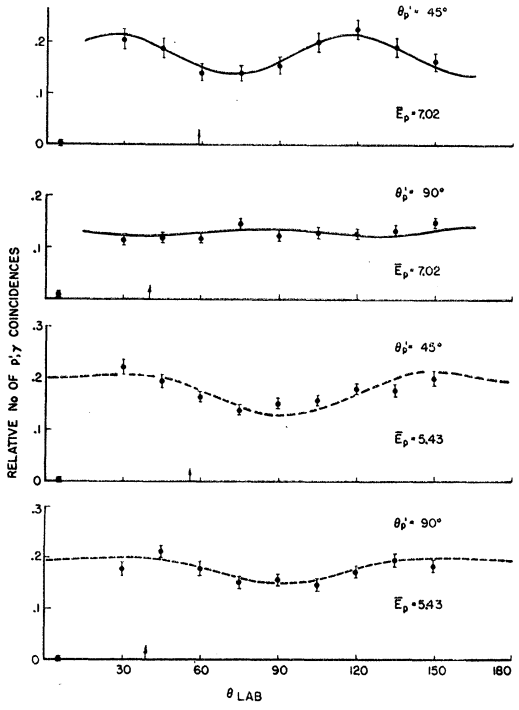

FIG. 10. $Cr^{52}(p,p'\gamma)$ angular correlations. Solid curves are of the form $A+B\sin^2(\theta_\gamma-\theta_0)$. Dashed lines are statistical-model predictions. Vertical arrows indicate recoil-nucleus direction.

Angular correlations are shown in Fig. 10. The statistical-model calculation at 5.43 Mev is shown as a dashed line. Optical-model T_L were used and the calculation includes only $L\leq 2$ and $L'\leq 2$. This includes about 85% of the reaction. These calculated correlations show no particular axis of symmetry. The main feature is the dip at 90° caused by the large $L=2$, $L'=0$ contribution. This minimum at 90° is also present in the experimental points. Correlations at 7.02 Mev have been fit with the DI form. This fit at $\theta_{p'}=45°$ is good but the axis of symmetry is not close to the recoil axis ($\theta_0=13°$) and the ratio of A/B is high. This probably indicates a large CN contribution to the reaction. The fit at $\theta_{p'}=90°$ is meaningless since the curve has almost no structure.

V. RESULTS—OTHER ELEMENTS

Angular distributions of inelastically scattered protons from other elements are shown in Figs. 11 and 12. The variation of $d\sigma/d\omega(90°)$ is shown in Figs. 4 and 11. This information for C can be found in the work of Brown and Lamarsh.[22]

The Be angular distribution is the only one which is well fitted by a spherical Bessel function. This fit, however, requires an unreasonably small nuclear radius. A more reasonable radius (dashed line) does not give a good fit. This angular distribution has the same shape at higher energy.[23]

The C angular distribution does not have the same shape as that of Gove and Stoddart at 7.26 Mev.[21] The Al angular distribution also changes form with a small change in energy. The variation of $d\sigma/d\omega(90°)$ and the change in shape of the angular distributions of these lighter elements with energy probably indicates a large level spacing in the CN. Thus the anisotropy of these angular distributions could be due to the fact that only a few CN levels contribute to the reaction. The isotropic Si angular distribution is probably an accident since $d\sigma/d\omega(90°)$ shows strong variations with energy.

Several Ti angular distributions were taken at energies <5.5 Mev. These were isotropic to about 10% and are not shown here. An Fe angular distribution was taken at 5.5 Mev and was also isotropic to about 10%. This is not shown because it contained an uncertain amount ($\sim$10%) of contamination from elastic scattering from C on the target. Because of this near isotropy, the Ti and Fe data in Fig. 4 have been compared with the statistical model total cross-section calculation. Solid lines correspond to black-nucleus T_L mentioned

[22] C. P. Brown and J. R. Lamarsh, Phys. Rev. **104**, 1099 (1956).
[23] R. G. Summers-Gill, Phys. Rev. **109**, 1591 (1958).

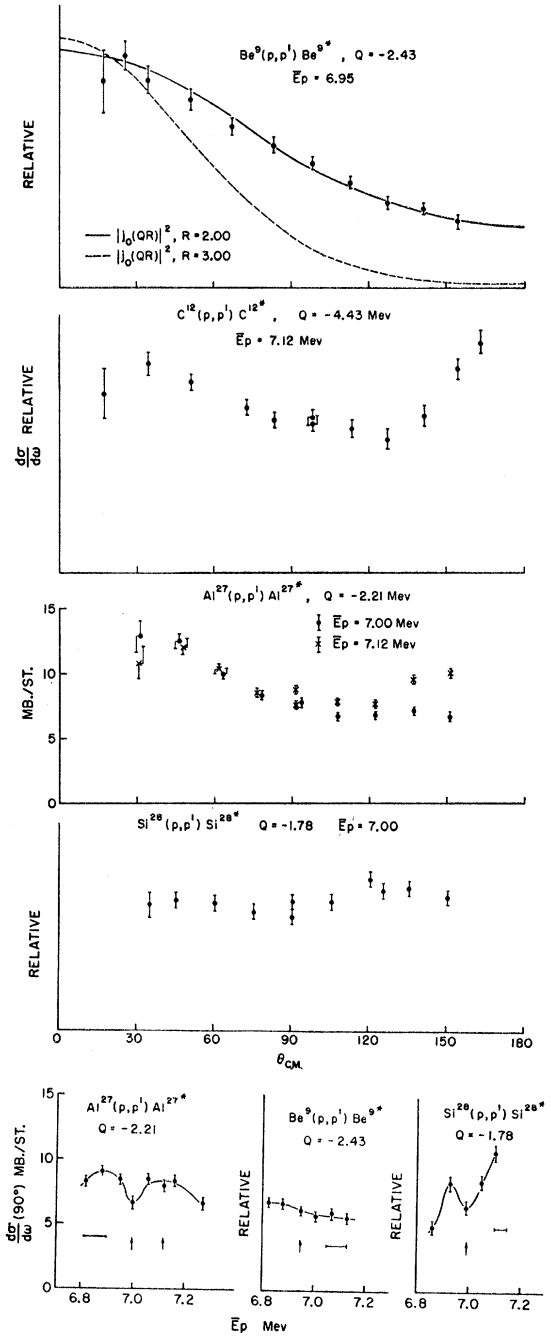

FIG. 11. Angular distributions of inelastically scattered protons and $d\sigma/d\omega$ (90°) for some of the lighter elements studied. Proton energies are lab energies. Solid lines drawn through the $d\sigma/d\omega$ (90°) points have no theoretical significance. Angular distributions have been converted to the center-of-mass system and the Born-approximation direct-interaction theory prediction for Be is shown as a dashed line.

previously. The dashed line on the Fe graph was computed using Preskitt's optical model phase shifts for Co^{59}.[18] The optical-well parameters were: $V=-63$ Mev, $W=-5$ Mev, $R=1.20A^{\frac{1}{3}}$ fermis, and $a=0.40$ fermi. This is a better fit than the black-nucleus calculation because the two-channel assumption should cause the calculated cross section to be too large as the energy increases.

It was not possible to resolve inelastically scattered protons from single states in V^{51} and Co^{59}. Estimates of $d\sigma/d\omega(90°)$ were made at several energies, however, and the cross section was found to be ~ 1 mb/sterad or less. No angular distribution measurements were possible with the present technique for cross sections this small. The smallness of these cross sections for odd-even targets compared with neighboring even-even targets is attributed to competition in the decay of the CN. Level spacing in the odd-even targets is smaller and the (p,n) threshold is lower (~ 1.5 Mev for Co^{59} and V^{51}). Thus there are more inelastic proton and neutron channels open for the decay of the CN formed by an odd-even nucleus and a proton.

VI. CONCLUSIONS

Much of these data can be interpreted by a CN (compound nucleus) mechanism. The variation of $d\sigma/d\omega(90°)$ and the shape of angular distributions with energy for the lighter elements is what one would expect if only a few CN levels were excited. The smoothing out of $d\sigma/d\omega(90°)$ with increasing Z and the trend toward isotropy of the angular distributions could be the effect of decreasing level spacing in the CN. The small (p,p') cross sections for odd-even targets and the leveling off of $d\sigma/d\omega(90°)$ just above the (p,n) threshold is well explained as a competition effect in the CN. The statistical model with T_L calculated on the basis of the optical model gives a good fit to the Cr data for proton energies up to 5.5 Mev.

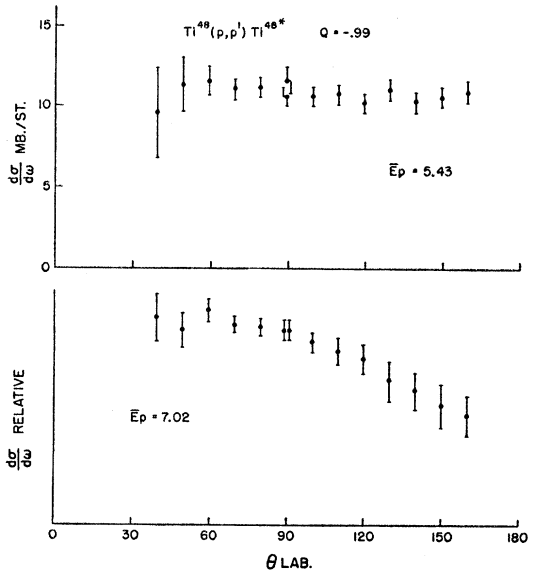

FIG. 12. Angular distributions of inelastically scattered protons leaving Ti^{48} in its first excited state. This data has been left in the lab system. It also contains a contribution of about 10% from the first excited state of Ti^{46}.

No angular distributions were found to be well fitted by spherical Bessel functions. This is not surprising since (a) there is probably a large CN contribution to the reaction at these energies, and (b) the Born approximation is probably not valid at energies this low. The Ti angular distribution shows a slight forward peaking at 7 Mev. This might be the start of a DI (direct interaction) since Ti data seemed to be isotropic up to this point, indicating that enough CN levels were excited so the statistical model was valid.

Angular correlations indicate that a large part of the $Mg^{24}(p,p')$ reaction may go by a DI at 7 Mev. Mg^{24} correlations at 5.4 Mev and Cr^{52} correlations at 7 Mev might be interpreted as having a bit of DI in them. Since no distorted wave DI calculations have been done at these energies, and since the CN contribution to the $Mg^{24}(p,p')$ reaction is unknown, these Mg angular correlations cannot be taken as proof of a DI. However, the form of the Mg correlations at 7.01 Mev is identical to DI predictions at higher energies, this form seems to be preserved when going through a resonance, and the $A+B\sin^2(\theta_\gamma-\theta_0)$ form gets "purer" as the energy increases. In view of this, plus the fact that Cr correlations are quite different at the same energies, it seems likely that a DI does form a large part of this $Mg^{24}(p,p')$ reaction.

The Coulomb barrier of the Mg nucleus is about 4 Mev high and that of the Cr nucleus is about 6 Mev high. All the experiments described are consistent with the assumption that the (p,p') reaction mechanism is predominantly compound nucleus formation when proton energies are below the barrier and direct interactions become appreciable as soon as the energy of both incident and scattered proton are well above the barrier.

VII. ACKNOWLEDGMENTS

The author wishes to express his appreciation to Professor W. P. Alford and to Dr. C. A. Preskitt, Jr. for many discussions and helpful suggestions concerning the experimental part of this work. Discussions with Professor J. B. French and Professor J. P. Elliott about the theory involved are also gratefully acknowledged.

VIII. APPENDIX

In this section, statistical-model expressions used to fit the (p,p') data of this paper are given. These expressions are probably only applicable to low-energy inelastic scattering of protons or neutrons from even-even nuclei. Some of these have been published[4,13] but contain errors. Since several experiments of this type are being done, and since a reasonable amount of work is necessary to obtain these expressions from the general formulas, it is felt that presenting them in this way is worthwhile.

These expressions are limited to low energies since only a few L and L' values are considered and since it is assumed that only two channels are open for the decay of the compound nucleus. L and L' refer to incident and scattered particle orbital angular momentum. The incoming and scattered particles both have spins of $\frac{1}{2}$, the target nucleus is 0^+ and the excited state is 2^+. The transmission coefficients or penetrabilities, T_L, must be calculated on the basis of some model. (The optical model was quite successful in fitting some of the data of this experiment.)

General expressions for the total and differential cross sections are given by Hauser and Feshbach.[11] For this special case, assuming that $T_L=0$ for $L>4$ and $T_{L'}=0$ for $L'>3$, these reduce to

$$\sigma=\tfrac{1}{2}\pi\lambda\!\!\!^{-2}\Big\{T_0\Big[\frac{2(2T_2')}{T_0+2T_2'}\Big]+T_1\Big[\frac{2(T_1'+T_3')}{T_1+T_1'+T_3'}+\frac{4(2T_1'+2T_3')}{T_1+2T_1'+2T_3'}\Big]+T_2\Big[\frac{10(T_0'+2T_2')}{T_2+T_0'+2T_2'}\Big]+T_3\Big[\frac{6(2T_1'+2T_3')}{T_3+2T_1'+2T_3'}+\frac{8(T_1'+2T_3')}{T_3+T_1'+2T_3'}\Big]+T_4\Big[\frac{8(2T_2')}{T_4+2T_2'}+\frac{10T_2'}{T_4+T_2'}\Big]\Big\}.$$

and

$$\begin{aligned}\frac{d\sigma}{d\omega}=\tfrac{1}{2}\lambda\!\!\!^{-2}\Big[&\frac{T_0T_2'}{T_0+2T_2'}+\frac{1}{2}\frac{T_1T_1'}{T_1+T_1'+T_3'}+\frac{1}{2}\frac{T_1T_3'}{T_1+T_1'+T_3'}\\&+\frac{T_1T_1'}{T_1+2T_1'+2T_3'}\Big(2-\tfrac{3}{5}P_2\Big)+\frac{T_1T_3'}{T_1+2T_1'+2T_3'}\\&\times\Big(2+\tfrac{3}{5}P_2\Big)+\frac{5}{2}\frac{T_2T_0'}{T_2+T_0'+2T_2'}+\frac{T_2T_2'}{T_2+T_0'+2T_2'}\\&\times\Big(5+\frac{25}{49}P_2-\frac{9}{14}P_4\Big)+\frac{T_3T_1'}{T_3+2T_1'+2T_3'}\\&\times\Big(3-\frac{6}{35}P_2\Big)+\frac{T_3T_1'}{T_3+T_1'+2T_3'}\Big(2+\frac{10}{7}P_2\Big)\\&+\frac{T_3T_3'}{T_3+2T_1'+2T_3'}\Big(3+\frac{31}{35}P_2-\frac{9}{7}P_4\Big)\\&+\frac{T_3T_3'}{T_3+T_1'+2T_3'}\Big(4+\frac{130}{63}P_2-\frac{120}{77}P_4-\frac{50}{99}P_6\Big)\\&+\frac{T_4T_2'}{T_4+2T_2'}\Big(4+\frac{50}{21}P_2-\frac{42}{49}P_4\Big)\\&+\frac{T_4T_2'}{T_4+T_2'}\Big(\frac{5}{2}+\frac{50}{21}P_2+\frac{15}{14}P_4\Big)\Big],\end{aligned}$$

where $P_L=P_L(\cos\theta)$.

TABLE I. Contributions of different L values to the $Cr^{52}(p,p')$ cross section at 5.43 Mev.

L	L'	$\sigma/4\pi$ mb/sterad	% contribution
0	2	0.88	6.5
1	1	2.35	17.7
1	3	0.06	0.5
2	0	6.21	46.5
2	2	2.37	17.8
3	1	0.81	6.1
3	3	0.03	0.2
4	2	0.63	4.7
Total		13.34	100.0

It is interesting to note the relative contribution of different L and L' values to these cross sections. Table I and Fig. 13 both refer to the reaction $Cr^{52}(p,p')Cr^{52*}$, $Q=-1.44$ Mev, $E_p=5.43$ Mev. The T_L are based on the optical model with parameters as given in Sec. IV. In Fig. 13 the contributions from different orbital angular momenta are shown to add to a nearly isotropic angular distribution. In Table I the relative contributions to the total cross section have been normalized to add to 100%. It seems likely, from the decrease in contribution with increasing L and L', that cutting off the calculation at $L=4$ and $L'=3$ includes 95% of the reaction or more.

General expressions for angular distribution of γ rays and angular correlations between inelastically scattered particles and γ rays have been derived by Devons and Goldfarb[12] and by Satchler.[4,13] For this special case, the angular distribution of γ rays, assuming $L\leq 4$ and $L'\leq 2$, becomes

$$W(\theta)=\frac{T_0T_2'}{T_0+2T_2'}(4)+\frac{T_1T_1'}{T_1+T_1'}(2)+\frac{T_1T_1'}{T_1+2T_1'}(8+2P_2)$$
$$+\frac{T_2T_0'}{T_2+T_0'+2T_2'}(10+5.430P_2-3.430P_4)$$
$$+\frac{T_2T_2'}{T_2+T_0'+2T_2'}(20-1.430P_2+1.715P_4)$$
$$+\frac{T_3T_1'}{T_3+T_1'}(8+4.075P_2-2.940P_4)$$
$$+\frac{T_3T_1'}{T_3+2T_1'}(12+4.645P_2+0.490P_4)$$
$$+\frac{T_4T_2'}{T_4+T_2'}(10+4.765P_2-3.890P_4)$$
$$+\frac{T_4T_2'}{T_4+2T_2'}(16+4.765P_2+2.285P_4),$$

where $P_L=P_L(\cos\theta)$.

If θ_2 and θ_3 are, respectively, the angles made by the inelastically scattered particle and the γ ray with the beam, and γ is the angle between the inelastically scattered particle and the γ ray, the angular correlation is[24]

$$W(\theta_2,\theta_3)=\frac{T_0T_2'}{T_0+2T_2'}[2+0.721P_2(\cos\gamma)+2.229P_4(\cos\gamma)]$$
$$+\frac{T_1T_1'}{T_1+T_1'}[1+0.500P_2(\cos\gamma)]+\frac{T_1T_1'}{T_1+2T_1'}$$
$$\times[4+P_2(\cos\theta_3)-2.800P_2(\cos\theta_2)$$
$$-2.000P_2(\cos\gamma)-0.535\Theta_{222}+0.383\Theta_{224}]$$
$$+\frac{T_2T_0'}{T_2+T_0'+2T_2'}[5+2.714P_2(\cos\theta_3)$$
$$-1.714P_4(\cos\theta_3)]+\frac{T_2T_2'}{T_2+T_0'+2T_2'}$$
$$\times[10-2.826P_2(\cos\gamma)-1.321P_4(\cos\gamma)$$
$$+1.974P_2(\cos\theta_2)-5.691P_4(\cos\theta_2)$$
$$-0.715P_2(\cos\theta_3)+0.852P_4(\cos\theta_3)$$
$$-1.026\Theta_{222}-0.213\Theta_{224}+0.091\Theta_{242}$$
$$-0.265\Theta_{244}+0.450\Theta_{422}+0.190\Theta_{424}$$
$$-0.604\Theta_{442}+0.112\Theta_{444}]$$

where

$$\Theta_{abc}=4\pi\left(\frac{2a+1}{2c+1}\right)^{\frac{1}{2}}\sum_m Y_b^{m*}(\theta_2,0)Y_c^m(\theta_3,\phi)(a0,bm|cm),$$

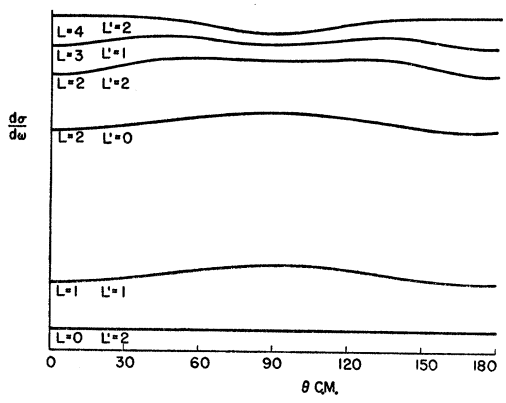

FIG. 13. Angular distribution of inelastically scattered protons leaving Cr^{52} in its first excited state as predicted by the statistical model. The calculation corresponds to a proton energy of 5.43 Mev and optical model penetrabilities were used. L and L' refer to the orbital angular momenta of incident and scattered protons, respectively.

[24] The author wishes to thank Dr. G. R. Satchler for correcting several errors in the author's original calculation.

$Y_l^m(\theta,\phi)$ are the usual spherical harmonics and $(am, bm'|cM)$ is a Clebsch-Gordan coefficient. Tables by Rose are useful in computing these Θ functions.[25]

Note that some terms in the above correlation are symmetrical about the beam direction and others are symmetrical about the direction of the inelastically scattered particle. Only $L \leq 2$ and $L' \leq 2$ are considered. Table I shows that this probably includes $\sim 85\%$ of the reaction. Higher L values were not considered because of the complexity of the calculation.

[25] M. E. Rose, Oak Ridge National Laboratory Report ORNL-2516, 1958 (unpublished).

PHYSICAL REVIEW VOLUME 114, NUMBER 2 APRIL 15, 1959

Elastic Scattering of 40-Mev Protons from Isotopes of Fe, Ni, and Cu†

MORTON K. BRUSSEL* AND JOHN H. WILLIAMS‡
University of Minnesota, Minneapolis, Minnesota

(Received November 26, 1958)

39.8-Mev protons were scattered from thin targets of Fe^{54}, Fe^{56}, Ni^{58}, Ni^{60}, and Cu^{65}. Absolute differential cross sections obtained with a statistical accuracy of $\leqq 3\%$ have been determined for the elastically scattered protons. The range of the angular distributions, 7.5° to 110°, encompassed three minima and three maxima in the measured cross sections. The energy resolution of the detection equipment, utilizing a NaI(Tl) crystal, was 1.2-2%. This enabled a separation to be made of elastic from nonelastic events. A detector telescope allowed angular resolutions of $\pm\frac{1}{8}°$ to be used in determining the shape of the features in the angular distributions. The general variation of the cross sections with the nuclear mass is noted. In addition, the data suggest that the nucleon shell closing about nucleon number 28 introduces fine structure differences in the shape and magnitude of features of the scattering pattern.

I. INTRODUCTION

MEASUREMENTS of angular distributions of protons elastically scattered from various elements provide one of the most amenable methods of determining nuclear force properties, since they give information about the shape and strength of the effective scattering potential active between proton and nucleus.

Burkig and Wright,[1] at 18.6 Mev, were the first to investigate nuclear effects of proton scattering in heavier elements. Although they missed the details present in the angular distributions, they did note that as the atomic number of their targets increased, the ratio of total elastic scattering differential cross sections to Rutherford scattering cross sections decreased.

Baker, Dodds, and Simmons[2] noticed at 10 Mev that specific features in the angular distribution of the elastically scattered protons tended to move towards smaller angles as the atomic number of the target nuclei increased. However, the first comprehensive study of proton elastic scattering differential cross sections was performed by Cohen and Neidigh[3] with 22-Mev protons. Plotting ratios of scattering differential cross sections to Rutherford scattering differential cross sections, they found systematic behavior of the features in the angular distributions as a function of atomic number, suggesting optical-like characteristics of nuclear matter.

The interest in elastic proton scattering generated by Cohen and Neidigh resulted in the accumulation of data from many other sources. The first accurate data, where elastically scattered protons were separated and distinguished from nonelastically scattered protons originating in the lowest excited states of the target elements, were compiled by Dayton[4] at 18 Mev. Here, due to greater energy resolution in the data, the scattering features were more pronounced. Only the elastic protons were counted; minima in the former data of Cohen and Neidigh were shallower due to nonelastic scattering contributions.

Subsequently much work has been done with protons in the energy interval 10–40 Mev. References to this work completed before 1957 can be found in the report of Hintz[5] for proton elastic scattering at 10 Mev. Higher energy elastic scattering data has been of more limited accuracy due to the inherently poorer energy resolution available with existing detection systems.

Measurements of proton elastic scattering have been mainly stimulated by the successes of the optical model, wherein a nucleus is represented as a partially absorptive ellipsoid. The most recent and comprehensive applications of this model to proton scattering have been made by Melkanoff,[6] Glassgold,[7] and their co-workers.

† This work was supported in part by the U. S. Atomic Energy Commission.

* Now at Brookhaven National Laboratory, Upton, New York.
‡ Now Director of Division of Research, U. S. Atomic Energy Commission, Washington, D. C.

[1] I. W. Burkig and B. T. Wright, Phys. Rev. **82**, 451 (1951).
[2] Baker, Dodds, and Simmons, Phys. Rev. **85**, 1051 (1952).
[3] B. L. Cohen and R. V. Neidigh, Phys. Rev. **93**, 202 (1954).
[4] I. E. Dayton, Phys. Rev. **95**, 754 (1954).
[5] N. M. Hintz, Phys. Rev. **106**, 1201 (1957).
[6] Melkanoff, Nodvik, Saxon, and Woods, Phys. Rev. **106**, 793 (1957).
[7] Glassgold, Cheston, Stein, Schuldt, and Erickson, Phys. Rev. **106**, 1207, (1957); A. E. Glassgold and P. J. Kellogg, Phys. Rev. **107**, 1372 (1957); Annual Progress Report, 1957–1958, University of Minnesota Linear Accelerator Laboratory, Minneapolis, Minnesota (unpublished).